JOURNAL OF SOLID STATE CHEMISTRY 135, 182–193 (1998)
ARTICLE NO. SC977619

Digital HREM Imaging of Yttrium Atoms in YB_{56} with YB_{66} Structure

Takeo Oku,[1] Anna Carlsson, L. Reine Wallenberg, Jan-Olle Malm, and Jan-Olov Bovin

National Center for HREM, Inorganic Chemistry 2, Chemical Center, Lund University, P.O. Box 124, S-221 00 Lund, Sweden

Iwami Higashi

The Institute of Physical and Chemical Research (RIKEN), Wako, Saitama 351-01, Japan

and

Takaho Tanaka and Yoshio Ishizawa

National Institute for Research in Inorganic Materials, Tsukuba, Ibaraki 305, Japan

Received February 14, 1997; in revised form September 9, 1997; accepted September 15, 1997

The arrangement of yttrium atoms in YB_{56} with YB_{66} structure was determined by high-resolution electron microscopy (HREM) using a slow-scan CCD camera. Digital HREM images recorded along the [100], [110], and [111] directions of the YB_{56} crystals showed "averaged" yttrium atom positions in the boron clusters, which were also confirmed by image simulation. Digital HREM images recorded from thin regions (< 5 nm) directly showed the local yttrium atom arrangements in the YB_{56}. In particular, the Y-hole, which consists of a single yttrium vacancy and a single yttrium atom, was detected in the boron clusters. The calculated images based on the proposed local structure model for yttrium atom arrangements agreed well with the observed images.

1. INTRODUCTION

Radiation-resistant monochromators, with high resolution in the 1–2 keV energy region, are required for soft X-ray synchrotrons. Gadolinium gallium garnet and beryl are used for monochromators because of the *d*-spacing of these materials. However, the crystal quality of these materials is low, and they suffer from synchrotron radiation damage. Recently, YB_{56} single crystals, with the YB_{66} structure, have been synthesized for use as high-resolution synchrotron-radiation-resistant monochromators (1). High quality YB_{56} single crystals can be grown with an incongruent composition, since this composition reduces the growth temperature compared to that for a congruent composition of [B]/[Y] = 62 (1, 2).

The YB_{66} compound was discovered by Seybolt (3), and its crystal structure was determined by Richards and Kasper (4). The crystal system of YB_{66} ($a = 2.3440$ nm) is cubic ($Fm3c$), and the composition ranges from YB_{33} to YB_{100} (5). After the discovery of the application of YB_{56} as a soft X-ray monochromator, the crystal structure of YB_{56} ($a = 2.34600$ nm) has been determined using single crystal X-ray diffractometry (6). The structure derived is shown in Fig. 1. The boron framework of YB_{56} is basically made of eight super-icosahedra $(B_{12})_{13}$ and eight nonicosahedral clusters (total of 1584 boron atoms). The YB_{56} has yttrium site occupancies of 0.575, which suggests that the peanut-shaped Y-hole (a pair of yttrium–yttrium sites) in the boron clusters should be occupied in most cases by only one yttrium atom (4–6). The structure of YB_{56-66} has been investigated by transmission electron microscopy (5), scanning tunneling microscopy (7), and atomic force microscopy (8). Scanning tunneling microscopy showed a periodicity of 1.2 nm, which indicates that there is no surface reconstruction at the YB_{66} surface (7). To our knowledge, no direct imaging of single yttrium atom positions in boron clusters has yet been done.

The purpose of the present work is to determine the yttrium atom arrangements in the YB_{56} crystal by digital high-resolution electron microscopy (HREM). HREM is a powerful method for direct observation of the atomic structures of advanced materials. Imaging plates (9, 10) and a slow-scan charge coupled device (CCD) camera (11–13), which have high linearity and electron sensitivity, are suitable tools for recording digital HREM images. In the present work, a slow-scan CCD camera was used to compare the observed images with the calculated images because of

[1]To whom correspondence should be addressed at the Institute of Scientific and Industrial Research, Osaka University, Mihogaoka 8-1, Ibaraki, Osaka 567, Japan.

0022-4596/98 $25.00

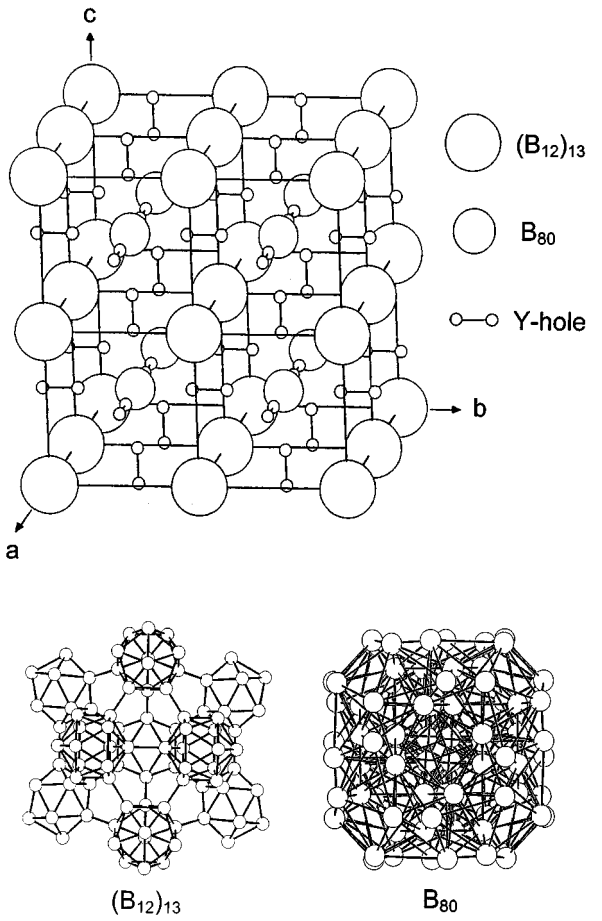

FIG. 1. Three-dimensional structure model of YB_{56}. Arrangement of $(B_{12})_{13}$ units, B_{80} clusters, and Y-holes.

the easy handling of digital data. From the observed digital HREM images, the averaged and local yttrium atom arrangements in the boron clusters in the YB_{56} crystal could be determined.

2. EXPERIMENTAL

High quality single crystals of YB_{56} were grown by an indirect heating floating-zone method (1, 2). The molten zone was heated by radiation from an inductively heated tungsten ring. The tungsten ring was placed between the work coil and the molten zone. A set of growth conditions for getting high quality YB_{56} single crystals is as follows: growth direction = [100], growth rate = 10 mm/h, rotation rate = 6 rpm (growth axis), atmosphere = He 0.3 MPa, composition of crystal [B]/[Y] = 56, and composition of the molten zone [B]/[Y] = 40.

Samples for HREM observations were prepared by dispersing crushed materials on a holey carbon grid. HREM observations were performed with a 400 kV electron microscope (JEM-4000EX) having a resolution of 0.16 nm. The electron microscope is equipped with a slow-scan CCD camera (Gatan SSC Model 694). The area of detection of the CCD camera is 1024×1024 pixels with a pixel size of $24 \times 24\,\mu m$. For image processing of the observed HREM images, Digital Micrograph (14) and Semper (15) software were used. As a first step, the digital images were masked and fast Fourier transformed. The reciprocal lattice was indexed, and the lattice parameters were determined using the positions of the strongest peaks in the transform. The local background is subtracted, and the amplitudes and phases of the peaks are refined using symmetrization (16, 17). Before the phases were corrected, the phase origin was determined by investigating the origin shift which best accorded with the phase conditions for the two-dimensional space group. Averaged symmetrized images were reconstructed from the corrected Fourier transform. To compare observed images with calculated ones, HREM images were produced by the multislice method (18, 19) using the Mac-Tempas software (20). The parameters used in the calculations are as follows: radius of the objective aperture = $6.3\,nm^{-1}$, spherical aberration $C_s = 1.0$ mm, spread of focus $\Delta = 8$ nm and semiangle of divergence $\alpha = 0.55$ mrad. The unit cell of the YB_{56} is fairly large (2.346 nm) for multislice calculation, the unit cell was subsliced into 4–8 layers for image calculation.

3. RESULTS AND DISCUSSION

3.1. Averaged Yttrium Atom Arrangements Observed from Three Directions

To observe the Y atom arrangements in the YB_{56}, three directions of the YB_{56} crystals were selected. Figure 2 shows HREM images of the YB_{56} taken along (a) [100], (b) [110], and (c) [111] directions using the slow-scan CCD camera. Cleavage planes of the YB_{56} crystals were {100} planes, which agree well with the growth planes of the YB_{56} crystal. To get an optimal resolution (< 0.016 nm/pixel), the digital images were recorded at microscope magnifications in the range of 1.0×10^6–1.2×10^6. The images were recorded close to Scherzer defocus. To observe the atomic arrangements clearly, image processing was carried out by using Fourier filtering, lattice averaging, and symmetrization. Figures 2a–2c are processed images of thin crystal (< 5 nm) along the (a) [100], (b) [110] and (c) [111] directions. Unit cells of YB_{56} ($a_0 = 2.346$ nm) are indicated by white lines, and yttrium atom positions with dark contrast are indicated by white arrows.

To investigate these "averaged" YB_{56} structure in detail, HREM images are calculated based on the structure model of YB_{56} determined by X-ray diffraction (6). Figure 3 shows simulated images (left) and projected structure models (right) of YB_{56} calculated along the (a) [100], (b) [110], and (c) [111] directions. Unit cells of YB_{56} are indicated by white lines, and yttrium atom positions with dark contrast

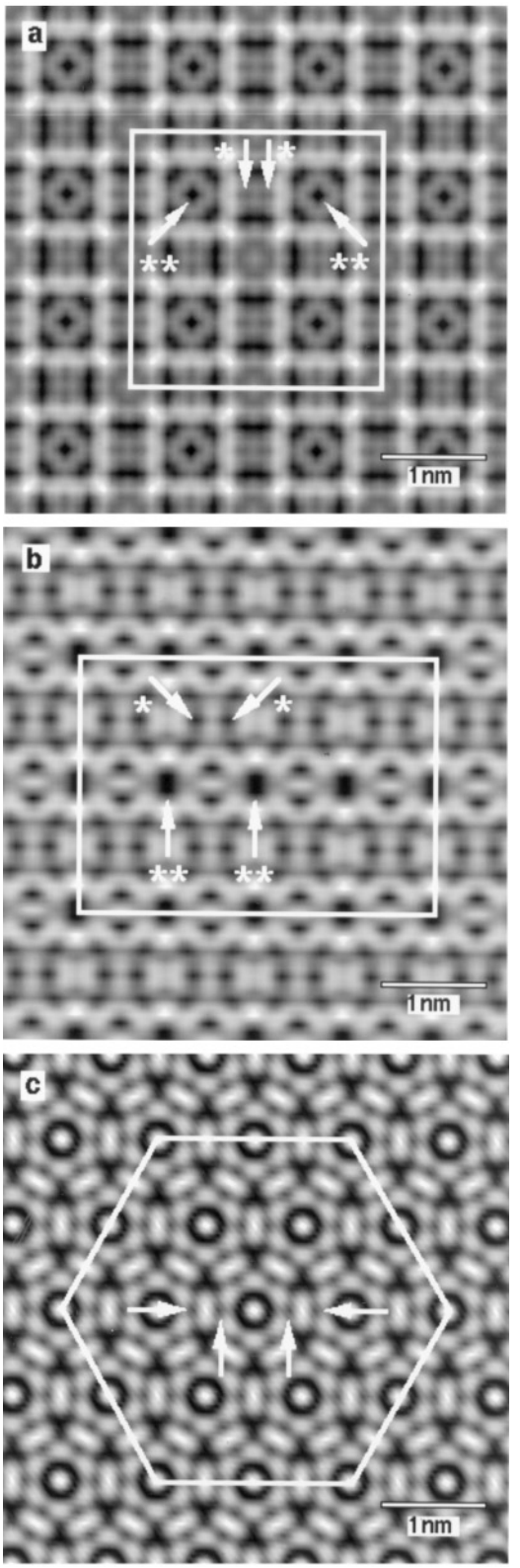

FIG. 2. Averaged experimental images of thin parts of the YB_{56} crystals: (a) [100], (b) [110], and (c) [111] incidences. Unit cells of YB_{56} are indicated by white lines. Yttrium atoms are indicated by white arrows.

are indicated by white arrows. The occupancy by yttrium atoms is 0.575. Image calculations were carried out for various defocus values and crystal thicknesses to determine the imaging condition. A defocus value of -45 nm (close to Scherzer defocus) and crystal thicknesses of (a) 2.35, (b) 3.32, and (c) 4.06 nm were selected as shown in Fig. 3. The comparison of processed images (Fig. 2) with calculated images (Fig. 3) is described in detail below.

In Fig. 2a, recorded along the [100] direction, the Y atom positions indicated by double asterisks show darker contrast compared to the other yttrium atom positions indicated by single asterisks, which agrees well with the calculated image of Fig. 3a. One set of two Y sites lies along [100] and one set of two sites is perpendicular to [100], thus giving twice as large a Y atom density along [100] for the former set. In the calculated image, the distance between yttrium atoms indicated by a single asterisk is 0.25 nm, which is different from the observed value of 0.16 nm. In addition, the contrast of yttrium atoms indicated by a single asterisk in the experimental image of Fig. 2a is fairly weak and dim compared to the calculated image of Fig. 3a. These results suggest that the yttrium atom is not fixed at only one position, and a detailed analysis of the yttrium atom positions will be described later.

Double rings with dark contrast are observed at the center and the corners of the marked unit cell in both processed (Fig. 2a) and calculated (Fig. 3a) images. Square-like rings with dark contrast are also observed around the yttrium atom positions indicated by double asterisks in Figs. 2a and 3a. These ring contrasts are due to boron clusters, as shown in the projected structure model of Fig. 3a.

For the [110] direction, two types of yttrium atom positions are observed in the unit cell as shown in the projected model of Fig. 3b. Although distances between yttrium atoms indicated by a single and double asterisks in the projected model are 0.272 nm and 0.192 nm, distances for corresponding yttrium atom contrasts in the calculated image of Fig. 3b are 0.18 and 0.26 nm, respectively. These contrast shifts of yttrium atoms are due to imaging conditions and the boron clusters around the Y-holes. In the processed image of Fig. 2b, only yttrium positions indicated by a single asterisk are separated. The darkness of yttrium atoms indicated by a single asterisk in the observed image of Fig. 2b are weak compared with the calculated image of Fig. 3b, which indicates a smearing of the yttrium atom positions. This will be explained in the next section. The boron clusters show dark contrast in the observed (Fig. 2b) and calculated (Fig. 3b) images.

For the [111] direction, yttrium atom positions appears as dark contrast in both observed (Fig. 2c) and calculated (Fig. 3c) images. Shortest distance of yttrium atoms in the projected plane is 0.192 nm, which is clearly separated in both images as indicated by white arrows. In the calculated

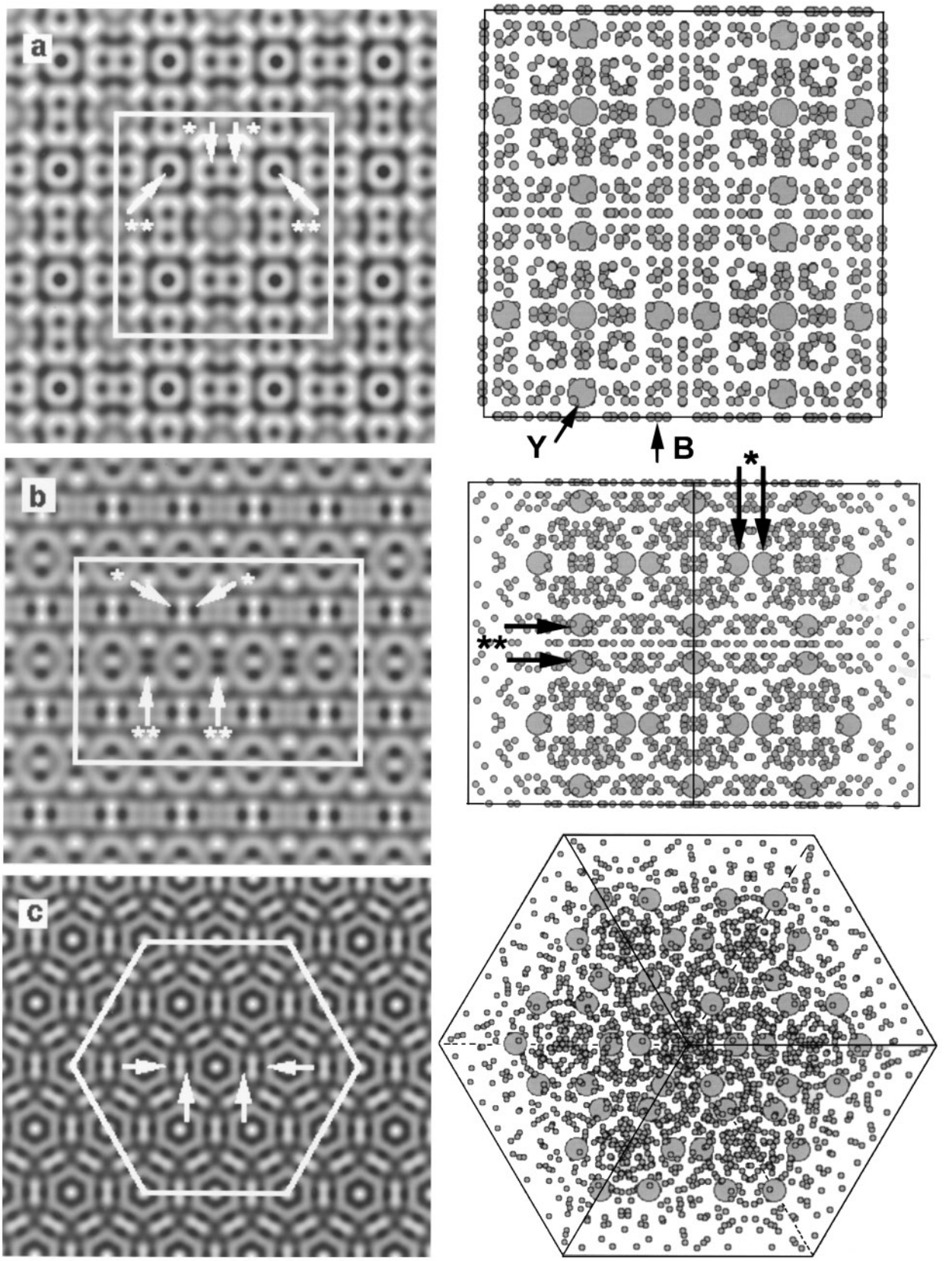

FIG. 3. Simulated HREM images (left) and projected structure models (right) of YB_{56} shown along the (a) [100], (b) [110], and (c) [111] directions. Unit cells of YB_{56} are indicated by white lines. The image calculations were carried out for a defocus value of -45 nm and a crystal thickness (depth of the projected model) of (a) 2.35, (b) 3.32, and (c) 4.06 nm.

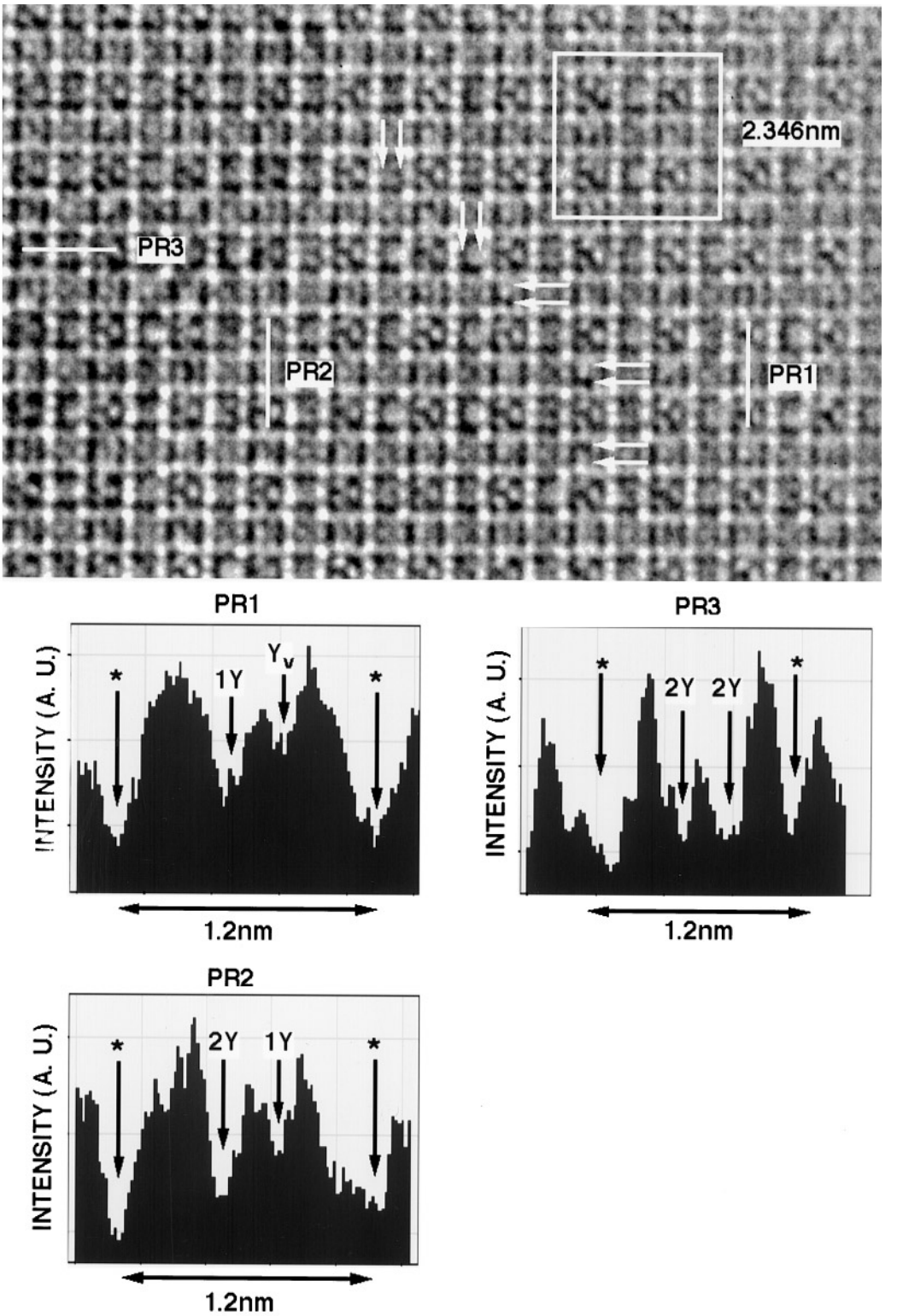

FIG. 4. Enlarged digital HREM image of thin part of a YB_{56} crystal observed along [100]. The unit cell of YB_{56} is indicated by a square (white lines). Line profiles (PR1, PR2, and PR3) of the recorded electron beam intensity (arbitrary units) are indicated below the HREM image.

image of Fig. 3c, the nearest yttrium atom distance is 0.21 nm, which agrees with the observed value of 0.21 nm. However, the darkness of the yttrium atom positions in the processed image of Fig. 2c is weak compared to the darkness of those in the calculated image of Fig. 3c, just as in the [100] and [110] direction. Boron clusters appear dark in both Fig. 2c and Fig. 3c.

Dark spots corresponding to yttrium atom positions in the averaged images recorded at thin regions from the three directions are weak compared to those of the calculated images. The yttrium site occupancy of 0.575, which was determined by X-ray diffraction, is merely a statistical value, but it implies that the Y-hole (the Y–Y pair with the shortest distance) might be occupied by only one yttrium atom. These results indicate alternating yttrium atom positions in the boron cluster from cell to cell, which will be described in the next section. The boron atom, which has a fairly low atomic number ($Z = 5$) compared to that of the yttrium atom ($Z = 39$), still shows dark contrast in both observed and calculated HREM images.

3.2. *Local Yttrium Atom Arrangement Observed along* [*100*]

As described in the previous section, the dark spots corresponding to yttrium atom positions were found to be comparatively weak in the averaged experimental images taken at the thin region (<5 nm). In this section, a local yttrium atom arrangement is investigated from the raw digital HREM image. Figure 4 is an enlarged HREM image of a thin part of the YB_{56} crystal. A unit cell of YB_{56} projected along [100] is indicated by a square (white lines). The yttrium atom positions (Y-holes) should show the same darkness, in principle, because of the equivalent sites. However, some of the Y-holes appear with different contrast, as indicated by double arrows. To measure the contrast, digital profiles (traces along PR1, PR2, and PR3) of the slow-scan CCD-recorded electron intensity were obtained. Right and left sides of the image are thin and thick regions of the YB_{56} crystal, respectively. Four minima indicated by Y_v, 1Y, 2Y, and asterisks are observed in all profiles. Different darknesses of Y-holes indicated by double arrows in Fig. 4 and different intensities of yttrium atoms in PR1 and PR2 would be due to different numbers of yttrium atoms.

To determine the number of yttrium atoms at the Y-holes along the observed [100] direction, a local model is proposed for yttrium atom arrangement, as shown in Fig. 5. The present model gives a suitable explanation for Y-holes, although other structural models might be considered. A unit cell of YB_{56} is divided into four layers (1L, 2L, 3L, and 4L) perpendicular to the [100] direction. In the 2L and 4L layers, there are 20 yttrium atom positions with site occupancies of 0, 0.575, and 1.0. Site occupancies of yttrium atoms in the 1L and 3L layers are all 0.575. Based on this local structure model of Fig. 5, HREM images were calculated at various thicknesses (1–10 nm), and some images are shown in Fig. 6. Stacking sequences for image calculations are shown above the calculated images. Line profiles of the image intensities are shown to the right of the images. Yttrium atom positions show dark contrasts and weak intensities. Since the yttrium atom positions show a reversed (bright) contrast at crystal thickness exceeding 5.8 nm, the image calculation was carried out for a crystal thickness of less than 5 nm. Positions of yttrium vacancy, one yttrium atom, and two yttrium atoms along the projected [100] direction are indicated by Y_v, 1Y, and 2Y, respectively.

The intensity profiles (PR1, PR2, and PR3) corresponding to yttrium positions in Fig. 4 are similar to those of Fig. 6. When the intensities of yttrium atom positions (Y-holes) are normalized to the intensities of yttrium atoms indicated by a single asterisk, it is possible to estimate the number of yttrium atoms along the [100] direction. (It was assumed that the Y atom positions indicated by a single asterisk have an averaged occupancy of 0.575.) The numbers of the yttrium atoms in the profiles of Fig. 4 were determined to be 0, 1, and 2 as indicated by Y_v, 1Y, and 2Y.

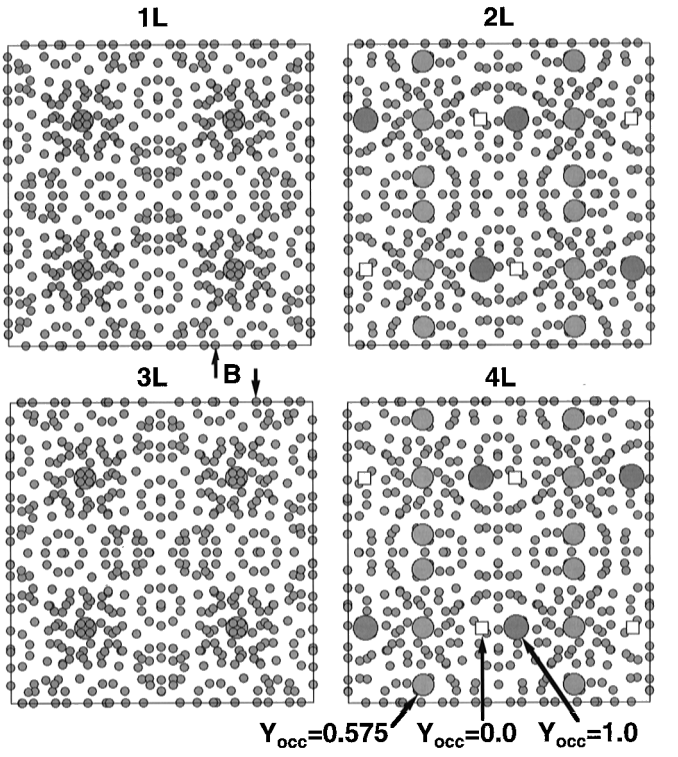

FIG. 5. Local atomic structure model of YB_{56} projected along [100]. The unit cell of YB_{56} is divided into four layers perpendicular to [100], shown here separated (1L, 2L, 3L, and 4L) perpendicular to [100]. Thickness (depth) of each layer is $1/4a_0 = 0.587$ nm. In the 2L and 4L layers, there are 20 yttrium atom positions with site occupancies (Y_{occ}) of 0, 0.575, and 1.0. Site occupancies of Y atoms in the 1L and 3L layers are all 0.575.

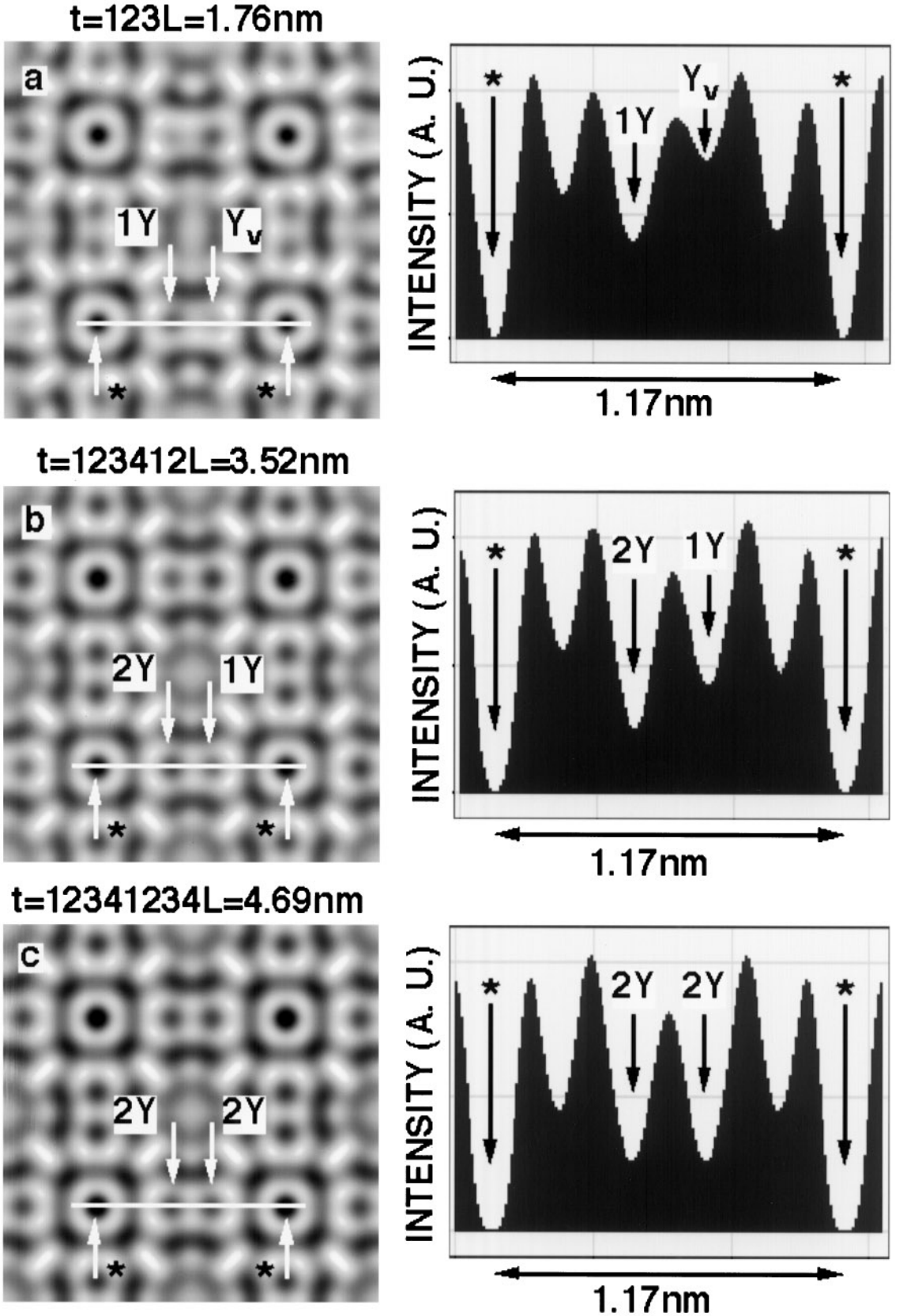

FIG. 6. Calculated images of YB_{56}, projected along [100], based on the local atomic structure model of Fig. 5. Stacking sequences from top of the crystal are shown above the calculated images. Crystal thicknesses are (a) 1.76, (b) 3.52, and (c) 4.69 nm. The defocus value is -45 nm. Line profiles of the image intensities are indicated at the right side of the images. Yttrium vacancy, one yttrium atom, and two yttrium atoms along the projected [100] direction are indicated by Y_v, 1Y, and 2Y, respectively.

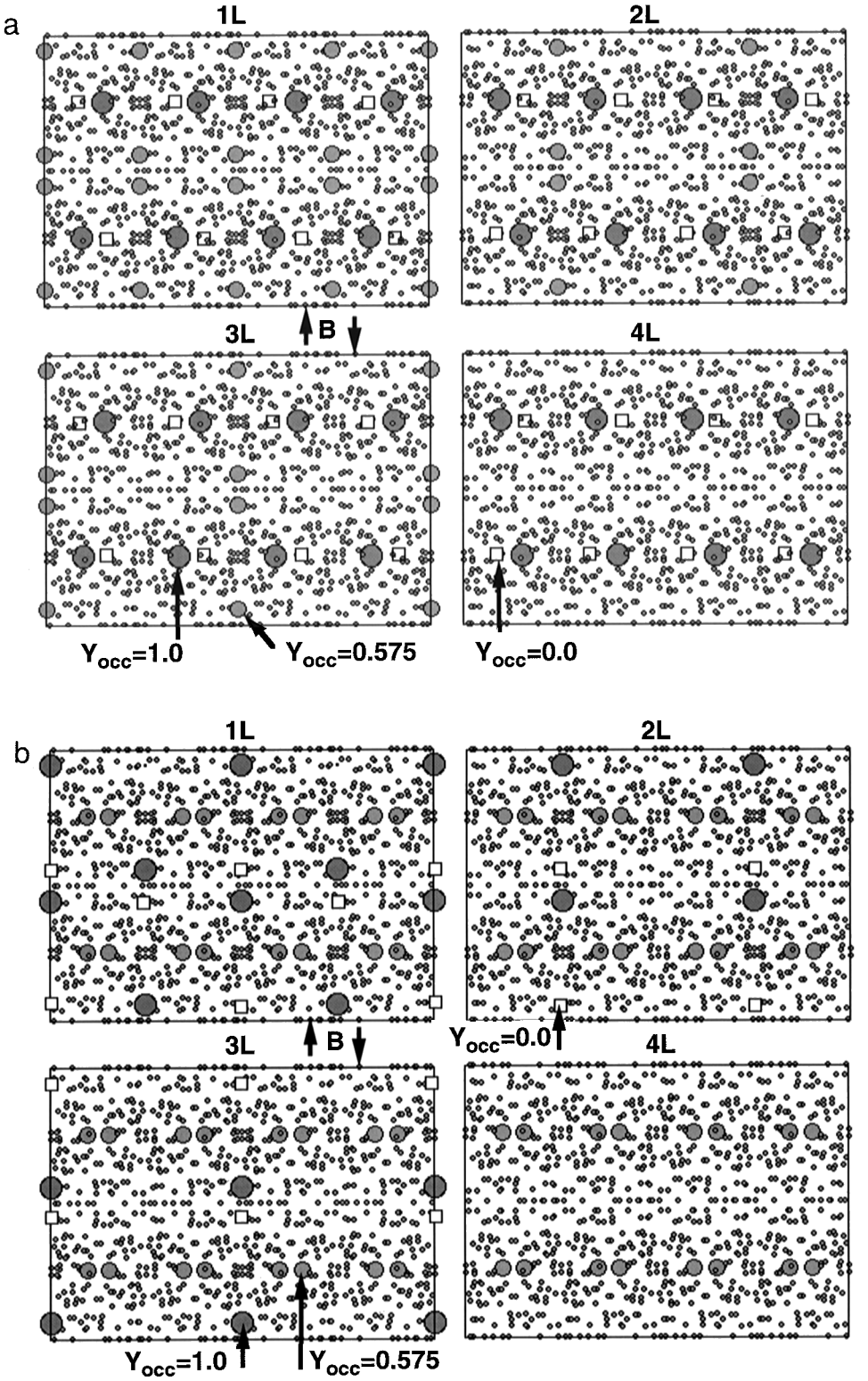

FIG. 7. Local atomic structure models of YB_{56} projected along ⟨110⟩: (a) [110] and (b) [−110] projection of Fig. 5. A projected unit cell of YB_{56} is divided into four layers perpendiculat to ⟨110⟩ (1L, 2L, 3L, and 4L). Thickness (depth) of each layer is 0.829 nm. There are three kinds of yttrium atom positions with site occupancies (Y_{occ}) of 0, 0.575, and 1.0.

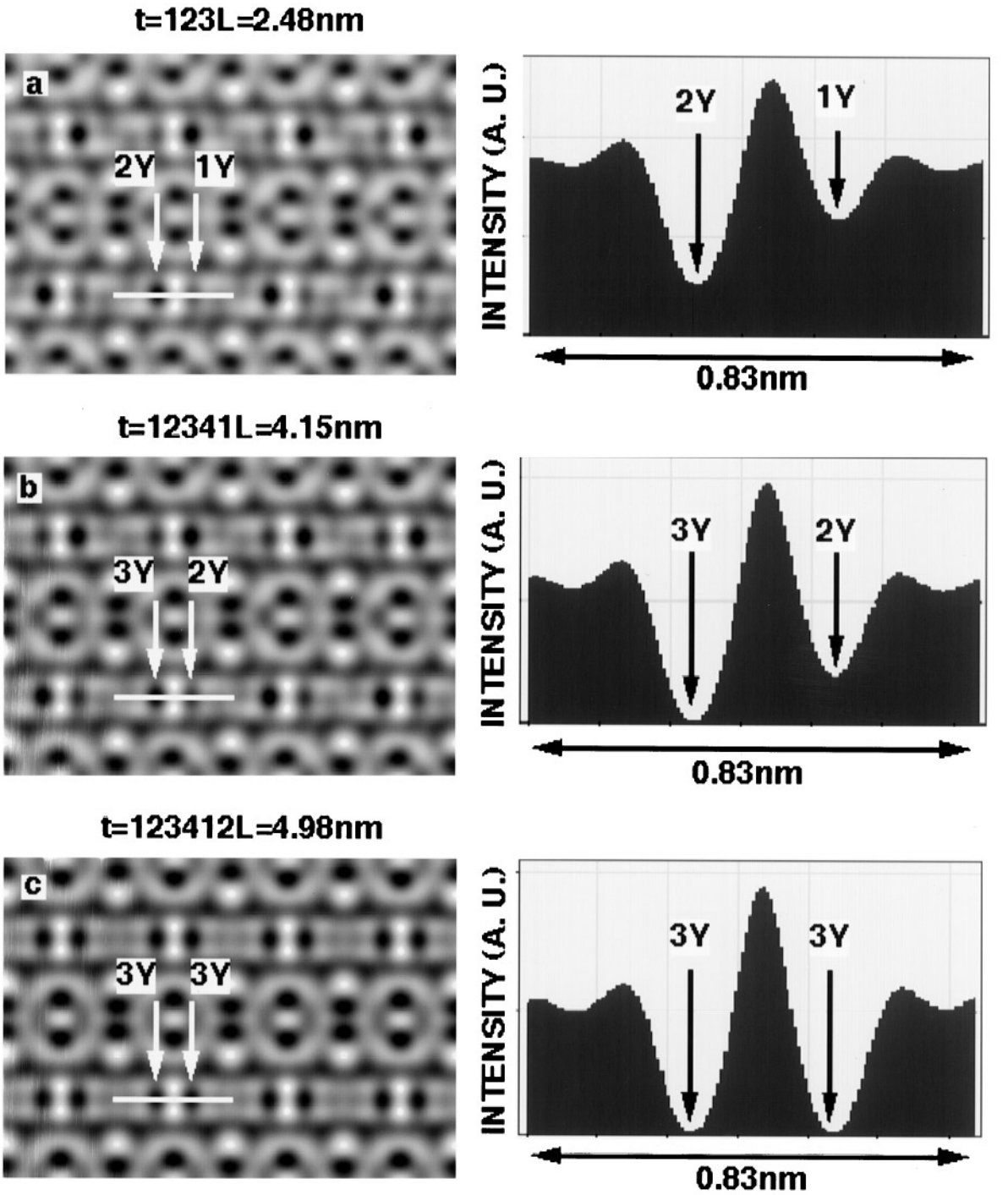

FIG. 8. Calculated images of YB_{56}, projected along [110], based on the local atomic structure model of Fig. 7a. The accumulated stacking sequences from top of the crystal are shown above the calculated images. Crystal thicknesses are (a) 2.48, (b) 4.15, and (c) 4.98 nm. The defocus value is -45 nm. Line profiles of the image intensities are indicated at the right side of the images. One, two, and three yttrium atoms along the projected [110] direction are indicated by 1Y, 2Y, and 3Y, respectively.

3.3. *Local Yttrium Atom Arrangement Observed along ⟨110⟩*

To confirm the local structure model of Fig. 5, calculations and observations along the ⟨110⟩ direction were carried out. Figures 7a and 7b are [110] and [−110] projections of the local structure model of Fig. 5. The unit cell of YB_{56} was divided into four layers (1L, 2L, 3L, and 4L) perpendicular to the ⟨110⟩ direction for the two projections. There are three types of yttrium atom positions in the divided layers with site occupancies of 0, 0.575, and 1.0. Based on the local structure model of Fig. 7, HREM images of YB_{56} projected along ⟨110⟩ are calculated as shown in Fig. 8 and Fig. 9. Stacking sequences are shown above the calculated images, and line profiles of the image intensities are shown to the right. Two yttrium atom positions (Y-holes) with different levels of dark contrast minima are clearly seen in Fig. 8 and Fig. 9.

Based on these projections and calculations from ⟨110⟩, the local yttrium atom arrangement projected along [110] was investigated from an unprocessed digital HREM image. Figure 10 is an enlarged digital HREM image of a thin YB_{56} crystal. The unit cell of YB_{56} projected along the [110] direction is indicated by white lines, and the yttrium atom positions appear dark. The yttrium atom positions (Y-holes) indicated by double arrows should show the same dark contrast if X-ray diffraction data are used. However, Y-holes with differing contrast at adjacent sites are observed and a few examples are indicated by double arrows. To quantify the contrast, line profiles (PR1, PR2, and PR3) of the recorded image intensities were extracted, and these are shown below the HREM image. Right and left sides of the image are thin and thick regions of the YB_{56} crystal, respectively. In the profiles (PR1, PR2, and PR3), the two minima in the intensity corresponding to yttrium atom positions are observed in all profiles, which agree well with the calculated profiles in Fig. 8. Normalizing the Y-hole intensity ratios at the profile edges of Fig. 8, the numbers of yttrium atoms were determined to be 1, 2, and 3, as indicated by 1Y, 2Y, and 3Y in Fig. 10.

The [−110] projection of Fig. 5 and the calculated images are shown in Fig. 7b and Fig. 9, respectively. At the thin region (2.48 nm) in Fig. 9a, Y-holes (pairs of Y_v and 1Y) show different darkness. At the thick region of 5.81 nm in Fig. 9b, two yttrium atoms are indicated by 2Y, and they all show the same darkness. Although these Y-holes are not perfectly resolved in Fig. 10, a difference in darkness could be observed. At the thin region, the Y-holes indicated by a single asterisk correspond to the features in the calculated image of Fig. 9a. At the thick region, the contrast of Y-holes indicated by double asterisks is closer to Fig. 9b. These results from observations and calculations confirm the proposed local structure model shown in Fig. 5 and Fig. 7.

From the HREM observation of YB_{56} in Fig. 4, the difference in occupancy of the Y-hole could be detected. The occupation of Y-holes is close to random when projected from longer distances in the [100] and [110] direction. When the Y-holes are formed, the cubic system is destroyed locally around them. However, it is difficult to determine the atomic arrangement of B around the Y-holes because of the low atomic number of boron. Higashi proposed B_{80} clusters around the Y-holes, but they have low boron atom occupancies (0.22–0.71) and large thermal parameters (0.017–0.058 nm^2) (6), which makes the determination more uncertain. The yttrium valence and the stability of the yttrium vacancy should be noted. One way to stabilize the yttrium vacancy is to insert boron at the vacant site.

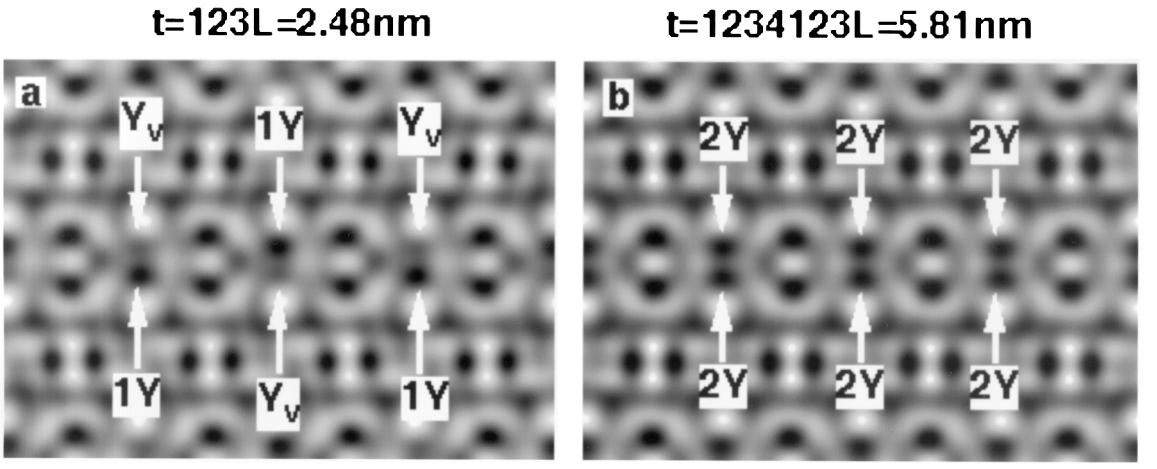

FIG. 9. Calculated images of YB_{56}, projected along [−110], based on the local atomic structure model of Fig. 7b. Stacking sequences from top of the crystal are shown above the calculated images. Crystal thicknesses are (a) 2.48, (b) 5.81 nm. The defocus value is −45 nm. Yttrium vacancies, one, and two yttrium atoms along the projected [−110] direction are indicated by Y_v, 1Y, and 2Y, respectively.

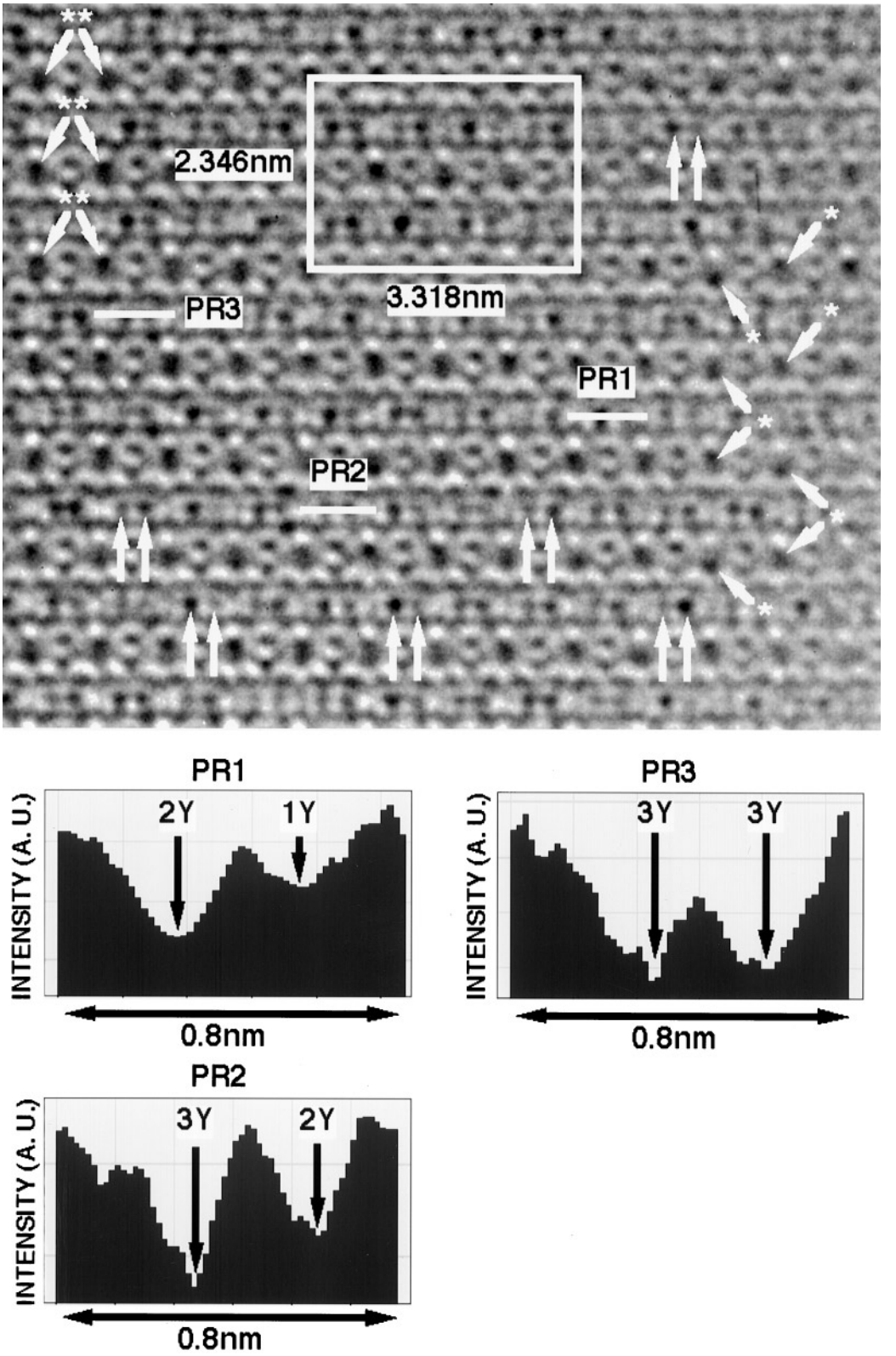

FIG. 10. Enlarged digital HREM image of thin part of the YB_{56} crystal observed along [110]. Unit cell of YB_{56} is indicated by a rectangle (white lines). Line profiles (PR1, PR2, and PR3) of the recorded image intensity (arbitrary units) are indicated below the HREM image.

The yttrium site occupancy of the YB_{56} is 0.575, which indicates that 15% of the Y-holes are occupied by two yttrium atoms simultaneously. When both yttrium sites are occupied, the distance between the yttrium atoms should be longer than 0.2716 nm, which is an average value from X-ray diffraction (6). However, a Y-hole with two yttrium atoms could not be clearly discriminated in the present work. The models proposed in the present study are not perfect, since there are three types of yttrium atoms with different occupancies. Although further work is needed on the Y-hole stability and boron cluster configuration around the Y-holes, this kind of structure determination would be useful for dopant site determination in compounds of, e.g., C_{60} clusters.

4. CONCLUSION

Arrangements and site occupancy of yttrium atoms in the YB_{56} crystals were directly determined by HREM using a slow-scan CCD camera. Digital HREM images recorded along [100], [110], and [111] directions of the YB_{56} crystals showed averaged yttrium atom arrangements inside the nonicosahedral boron cluster. The dark contrast of yttrium atom positions at the thin crystal regions in the averaged observed images is smeared compared to that of calculated images based on X-ray data, which indicates nonuniform yttrium atom distribution. Although boron has a fairly low atomic number compared to the yttrium atom, boron clusters also show dark contrast in both observed and calculated HREM images at a defocus of -45 nm. Digital HREM images of regions thinner than 5 nm directly showed local yttrium atom arrangements in the boron cluster. In particular, the Y-hole, which consists of a single yttrium vacancy and a single yttrium atom, was directly imaged and quantified. A local structure model for yttrium atom arrangements was proposed, and calculated images based on this model agreed well with observed images.

ACKNOWLEDGMENTS

The authors thank Christer Jönsson and Gunnel Karlsson for technical support and critical reading of the manuscript. T.O. and A.C. thank the Swedish Natural Science Research Council (NFR) for financial support.

REFERENCES

1. T. Tanaka, Y. Ishizawa, J. Wong, Z. U. Rek, M. Rowen, F. Schäfers, and B. R. Muller, *Jpn. J. Appl. Phys.* **10,** 110 (1994).
2. K. Kamimura, T. Tanaka, S. Otani, Y. Ishizawa, Z. U. Rek, and J. Wong, *J. Cryst. Growth* **128,** 429 (1993).
3. A. U. Seybolt, *Trans. Am. Soc. Met.* **52,** 971 (1960).
4. S. M. Richards and J. S. Kasper, *Acta Crystallogr.* **25,** 237 (1969).
5. G. A. Slack, D. W. Oliver, G. D. Brower, and J. D. Young, *J. Phys. Chem. Solids* **38,** 45 (1977).
6. I. Higashi, K. Kobayashi, T. Tanaka, and Y. Ishizawa, submitted for publication.
7. C. L. Perkins, M. Trenary, and T. Tanaka, *Proc. Int. Symp. Boron Borides Relat. Compounds* **12,** 19 (1996).
8. U. Kuhlmann, H. Werheit, T. Tanaka, and Y. Ishizawa, *Proc. Int. Symp. Boron Borides Relat. Compounds* **12,** 69 (1996).
9. A. Tokiwa, T. Oku, M. Nagoshi, D. Shindo, M. Kikuchi, T. Oikawa, K. Hiraga, and Y. Syono, *Physica C* **172,** 155 (1990).
10. D. Shindo, T. Oku, J. Kudoh, and T. Oikawa, *Ultramicroscopy* **54,** 221 (1994).
11. M. Pan and P. A. Crozier, *Ultramicroscopy* **52,** 487 (1993).
12. Y. Sasaki, T. Suzuki, Y. Ikuhara, and A. Saji, *J. Am. Ceram. Soc.* **78,** 1411 (1995).
13. N. Ohnishi and K. Hiraga, *J. Electron Microsc.* **45,** 85 (1996).
14. Gatan, Inc., California.
15. Synoptics Ltd., Cambridge, UK.
16. S. Hovmöller, A. Sjögren, G. Farrants, M. Sundberg, and B.-O. Marinder, *Nature* **331,** 238 (1984).
17. A. Carlsson, *in* "Proceedings European Congress on Electron Microscopy, Spain, 1992," p. 497.
18. J. M. Cowley and A. F. Moodie, *Acta Crystallogr.* **10,** 609 (1957).
19. J. M. Cowley, "Diffraction Physics", 2nd rev. ed. North-Holland, Amsterdam, 1981.
20. Total Resolution, California.